Commissioning of electron cyclotron emission imaging instrument on the DIII-D tokamak and first data

Commissioning of electron cyclotron emission imaging instrument on the DIII-D tokamak and first data[a)]

B. Tobias,[1,b)] C. W. Domier,[1] T. Liang,[1] X. Kong,[1] L. Yu,[1] G. S. Yun,[2] H. K. Park,[2] I. G. J Classen,[3] J. E. Boom,[3] A. J. H. Donné,[3,4] T. Munsat,[5] R. Nazikian,[6] M. Van Zeeland,[7] R. L. Boivin,[7] and N. C. Luhmann, Jr.[1]
[1]*University of California at Davis, Davis, California 95616, USA*
[2]*Pohang University of Science and Technology, Pohang, Gyeongbuk 790-784, Korea*
[3]*FOM-Institute for Plasma Physics Rijnhuizen, 3430 BE Nieuwegein, The Netherlands*
[4]*Eindhoven University of Technology, 5600 MB Eindhoven, The Netherlands*
[5]*University of Colorado, Boulder, Colorado 80309, USA*
[6]*Princeton Plasma Physics Laboratory, Princeton, New Jersey 08543, USA*
[7]*General Atomics, San Diego, California 92121, USA*

(Presented 18 May 2010; received 10 May 2010; accepted 26 May 2010; published online 28 October 2010)

A new electron cyclotron emission imaging diagnostic has been commissioned on the DIII-D tokamak. Dual detector arrays provide simultaneous two-dimensional images of T_e fluctuations over radially distinct and reconfigurable regions, each with both vertical and radial zoom capability. A total of 320 (20 vertical $\times$ 16 radial) channels are available. First data from this diagnostic demonstrate the acquisition of coherent electron temperature fluctuations as low as 0.1% with excellent clarity and spatial resolution. Details of the diagnostic features and capabilities are presented. © *2010 American Institute of Physics.* [doi:10.1063/1.3460456]

I. INTRODUCTION

Cyclotron emission from electron populations in high temperature plasma experiments is harnessed for diagnostic purposes yielding insight into a wide variety of plasma phenomena. Under conditions of favorable optical thickness, two-dimensional (2D) measurements of electron temperature may be obtained using electron cyclotron emission imaging (ECEI) techniques[1–6] with high spatial and temporal resolution limited only by diffraction and the dependence of statistical noise on video and intermediate frequency (IF) bandwidths.[7] When plasma temperature is sufficiently high as to result in low electron collisionality and highly adiabatic electron population behavior, fluctuations in electron temperature may be readily related to field line perturbations or perturbations in energetic ion populations.[8,9] Furthermore, in regions of low optical thickness, the dominance of density dependence on ECE transmission may be made use of to characterize density fluctuations.[10] Therefore, ECE diagnostics find a wide variety of applications in obtaining electron temperature profiles, resolving temperature fluctuations over a broad range of scale lengths and frequencies, imaging magnetohydrodynamic (MHD) activity such as tearing modes, sawteeth, and Alfvén eigenmodes, and characterizing activity in the plasma edge and pedestal regions.

In this paper, details of the features and capabilities of a newly commissioned dual-array ECEI diagnostic for the DIII-D tokamak are presented. First data from this instrument provide new images of MHD activity near the plasma core, including the first 2D images of Alfvén eigenmode activity on DIII-D. ECEI is deployed as a fully realized diagnostic technique, poised to provide new physical insights into the behavior of tokamak plasmas.

II. OVERVIEW OF THE DIII-D ECEI SYSTEM

The DIII-D ECEI system, as installed at the 270° midplane port of the DIII-D tokamak, is shown in Fig. 1. This so-called man-hole port of the vessel allows for utilization of a large aperture fused silica window which accommodates diffractive spreading such that 1 cm full-width half maximum resolution of the viewing beams may be achieved without significant clipping from port apertures. Large aperture zoom optics are remotely configurable and provide variable vertical plasma coverage of up to 55 cm. Dual objective lens systems control the focusing of the imaging arrays which are combined by a thin-film dielectric beamsplitter. 2–18 GHz IF signals are carried by coaxial cable to remotely located IF electronics, where final downconversion, video filtering, detection, and digitization of the 0–400 kHz signals are performed.

The high performance optical coupling scheme employed in this system provides vertical zoom at a greater than 2:1 ratio, while the focal region of the viewing detectors may be independently translated from the plasma edge to regions well within the high field side of the plasma core. This flexibility allows the diagnostic to obtain localized measurements for toroidal magnetic field in the range of 1.5–2.1 T, covering the typical of operating scenarios at DIII-D. High

[a)]Contributed paper, published as part of the Proceedings of the 18th Topical Conference on High-Temperature Plasma Diagnostics, Wildwood, New Jersey, May 2010.
[b)]Author to whom correspondence should be addressed. Electronic mail: bjtobias@ucdavis.edu.

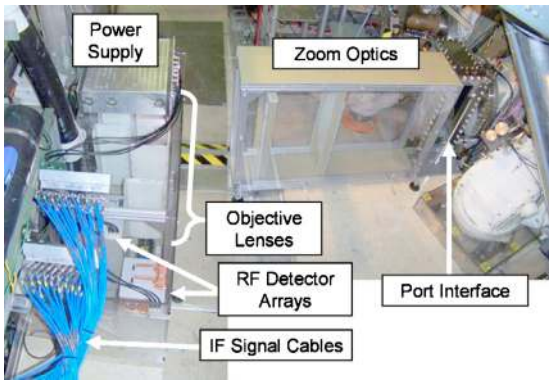

FIG. 1. (Color online) The DIII-D ECEI system is shown installed at the 270° midplane port. A thin-film dielectric beamsplitter combines high (90–140 GHz) and low (75–85 GHz) frequency systems so that common vertical zoom optics may be used in conjunction with separate objective lenses for independent radial focusing at like vertical coverage. 2–18 GHz IF signals generated at the two rf detector array modules are carried by shielded coaxial cable to the IF electronics, outside the experiment hall and shielded from exposure to stray radiation.

resolution laboratory characterization of the optical coupling system, as illustrated in Fig. 2, reveals excellent agreement with simulation. Spot sizes of the viewing beams vary with the vertical zoom and range from 1.5 to more than 3 cm. In a high resolution configuration, the diagnostic is sensitive to fluctuations with k_θ up to 2.1 cm^{-1}. Conversely, a wide zoom configuration results in focal depths of up to 100 cm.

Two separate 20 vertical $\times$ 8 radial = 160 channel arrays comprise the detector section of the DIII-D ECEI diagnostic. Coupled to separate LO sources, one being a backward wave oscillator (BWO) tunable over a full waveguide band, and the other a fixed frequency Gunn oscillator, imaging may be performed at any radial position corresponding to second harmonic ECE radiation from 75 to 140 GHz. Future upgrades will make use of two BWO sources, allowing further flexibility. For protection, both sources are located outside

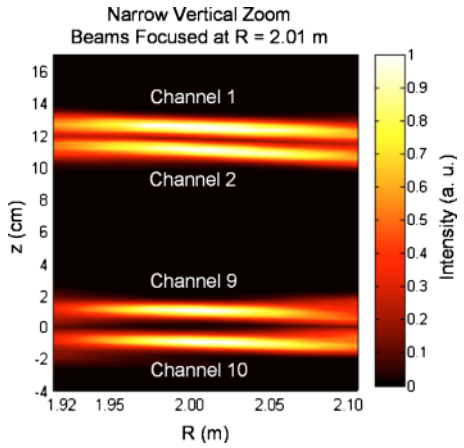

FIG. 2. (Color online) Laboratory characterization of the optical coupling system is performed using a millimeter wave scattering source as described in Ref. 1. A composite image shows the positions, sizes, and qualities of beam waists formed by edge and center channels of the system. Comparison with full-wave diffractive simulation of the optics reveals an agreement in these parameters to within the resolution of the measurement, typically 0.5 mm vertical and 5 mm horizontal.

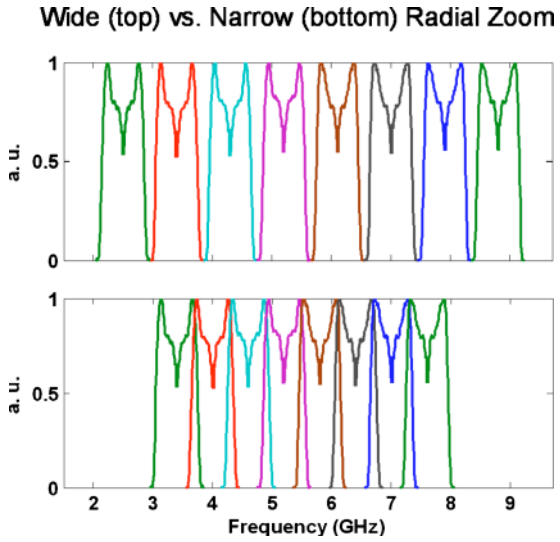

FIG. 3. (Color online) The frequency response of each rf channel, or line of sight, is plotted to illustrate the bandwidth and relative center frequencies of the IF channels. IF channel spacing may be switched from 900 to 600 MHz resulting in 1.5:1 radial zoom. IF bandwidth (700 MHz) and video bandwidth (variable from 12.5 to 400 kHz) are unaffected by this feature. The notch seen at the center of each IF passband rejects the voltage controlled oscillator signal used in the final downconversion step. Single sideband mixing of the rf signal ensures that each channel corresponds to a single localized plasma region.

the experiment hall and coupled to the detector arrays by low loss corrugated waveguide and LO coupling optics.

Quasioptical high pass filters ensure single sideband mixing such that any 7 GHz (approximately 10–15 radial cm, depending on location) span is subdivided into eight distinct frequency channels by a double-downconversion process as described in Ref. 2. A new feature of radial zoom is implemented on the DIII-D ECEI system, whereby the radial channel spacing may be switched between 900 and 600 MHz, as shown in Fig. 3. For 1.75 T operation, this corresponds to switching between 8.5 and 12.75 cm of radial coverage at the plasma center.

III. ADVANCED IMAGING DETECTOR ARRAYS

Two detector arrays, containing 20 antennas each (with accommodation for 24 channels in future upgrades), are operated simultaneously in the DIII-D ECEI system. In a novel approach first described in Ref. 11, a beamsplitter is mounted inside each detector array module to achieve front-side coupling of LO power without the use of a beam dump, while doubling the channel density of the image. Two arrays of ten dual-dipole antennas are fitted with Schottky mixing diodes and coupled to 1 in. miniature substrate lenses.[12] One array is positioned at the LO reflection (rf transmission) side of the internal beamsplitter, the other at the LO transmission (rf reflection) side. Both arrays are equally illuminated with rf signal and LO power and imaged to the same toroidal plasma location. This allows for a 3 dB improvement in the efficiency of LO coupling, while allowing for a doubling of the vertical image sampling over limitations imposed by the physical sizes of the substrate lenses.

A single detector module is shown, along with examples of the planar quasioptical filter components used in the ECEI

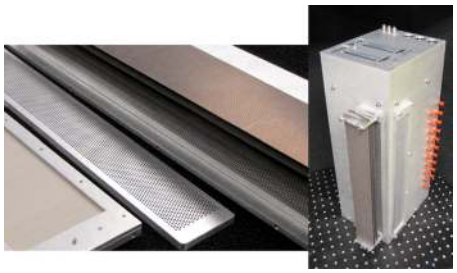

FIG. 4. (Color online) Quasioptical planar filter components and an assembled imaging detector array are shown. From left to right: 3 dB thin-film dielectric beamsplitter, 115 GHz dichroic plate (high pass filter), and 110 GHz notch filter assembly (60 dB rejection). The detector array shown is approximately 35 cm in height and shown configured for acquisition of ECE signals from 77 to 105 GHz during ECH operation. Containing detector bias circuitry and 25 dB gain low noise IF amplifiers, it is fully enclosed and electromagnetically shielded, allowing it to be operated very near the tokamak without adverse electrical pickup.

system, in Fig. 4. The array module is reconfigurable for operation anywhere in the 75–140 GHz range of the diagnostic, and may be fitted with 110 GHz ECH notch filters. Normal operation of the ECEI diagnostic has been demonstrated in L-mode plasmas for ECH powers up to 3.5 MW. 60 dB of 110 GHz isolation ensures that the diagnostic not only obtains appropriate temperature profiles during normal operations but is also protected from damage in overdense sce-

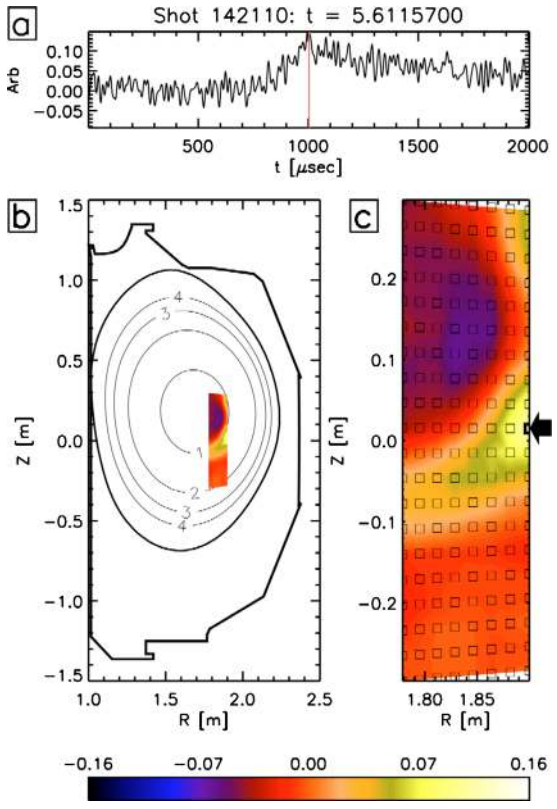

FIG. 5. (Color online) The time trace of a single reference channel [indicated by the black arrow in (c)] identifies a fluctuation in the local electron temperature (a), defined as $\tilde{T}_e/\langle T_e\rangle$. The viewing range of a single complete detector array is shown overlaid on a reconstruction of the equilibrium plasma flux surfaces with local q contours indicated (b) and enlarged to show detail (c). A magnetic island near the $q=1$ surface is identified as it passes through the field of view of the diagnostic. The second detector array (not shown) acquires data over a comparable region.

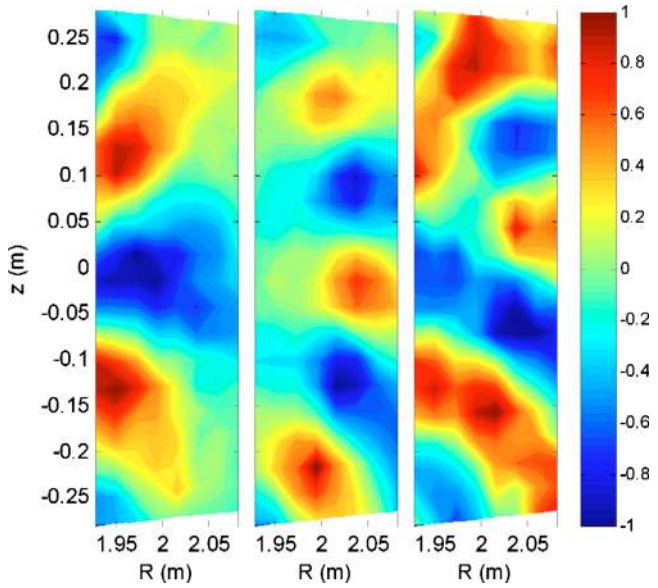

FIG. 6. (Color online) Alfvénic activity from shot No. 142111 is imaged during selected Fourier transform windows and scaled as $\tilde{T}_e/|\tilde{T}_e|$, where the relative magnitude of the fluctuation is approximately 1% (100 eV) for each of the modes shown. At t=560.85 ms, a RSAE mode is identified oscillating at 82.031 kHz (left). The frequency of this mode has a strong dependence on the q profile, and hence it chirps upward as time progresses. A second mode is observed to oscillate at 87.89 kHz (middle). This mode has a higher poloidal mode number, m, and is observed to chirp down over time. At t=564.36 ms, these modes intersect in frequency space at 85.449 kHz (right). Weakly coupled due to their differing radial localization (Ref. 13), their behavior integrated over a 366 Hz window may be described as a superposition of the constituent modes. Regions of both constructive and destructive interference are observed in the view of the ECEI diagnostic.

narios or losses of plasma confinement during which intense ECH power may be reflected through the ECEI port.

IV. FIRST DATA AND INITIAL RESULTS

Successful operation of the ECEI system through March of 2010 demonstrates the unique capabilities of this diagnostic. An example of the available plasma coverage relative to the poloidal cross section of the DIII-D tokamak (for one particular configuration) is given in Fig. 5. In this still frame, a magnetic island is visible as it passes through the view of the diagnostic. When operated simultaneously, a second image of comparable extent may be acquired to either side of the image shown. Remote control of LO frequency, lens configuration, and dichroic plate selection will allow the size and position of each image to be varied on a shot-by-shot basis from the DIII-D control room during experiments in 2011.

The first 2D images of Alfvén eigenmode activity on DIII-D provide an exciting glimpse into the capability of this new diagnostic. Both toroidicity induced and reverse shear induced Alfvén eigenmodes (RSAEs) below the 0.1% fluctuation level are readily imaged with remarkable clarity. An example of the Alfvénic behavior is given in Fig. 6, where successive time windows of 1.5–3 ms are Fourier decomposed in order to illustrate behavior in discrete frequency intervals. An interesting 2D structure is revealed which both complements observations made by one-dimensional ECE radiometry[8] and provides new information that remains to be

evaluated. It is clear from these images that localized core measurements, such as those provided by ECE diagnostics, have inherent advantages over line-integrated measurements or magnetic measurements made external to the plasma. Many of the modes observed by ECEI are either deep in the plasma where magnetic probes are ineffective, or exhibit complicated radial structure that may easily be misinterpreted or underrepresented by line-integrated diagnostic techniques such as interferometry or soft x-ray observations.

V. CONCLUSION

A new and highly flexible ECEI diagnostic has been installed on the DIII-D tokamak and first data demonstrate its utility in the characterization of plasma fluctuations and MHD behavior. A wide variety of plasma phenomena have been recorded, only a few examples of which are presented here. Future upgrades will enhance the capabilities of the diagnostic, enabling it to be more efficiently utilized in a variety of experiments during the coming experimental campaign.

ACKNOWLEDGMENTS

This work was supported by the U.S. DOE (Grant Nos. DE-FG02-99ER54531, DE-FG02-05ER54816, DE-AC02-09CH11466, and DE-SC0003913), NWO, POSTECH, and the association EURATOM-FOM. The authors would like to extend their thanks to Mark Smith and the entire PPPL team, to Jim Kulchar and the DIII-D diagnostics group, and to Professor William Heidbrink for their valuable contributions. In addition, the authors are immensely grateful to all members of the UC Davis Plasma Diagnostics Group without their tireless work, this project would not have been possible.

[1] B. Tobias, X. Kong, T. Liang, A. Spear, C. W. Domier, N. C. Luhmann, Jr., I. G. J. Clssen, J. E. Boom, M. J. van de Pol, R. Jaspers, A. J. H. Donné, H. K. Park, and T. Munsat, Rev. Sci. Instrum. **80**, 093502 (2009).
[2] C. W. Domier, Z. G. Xia, P. Zhang, N. C. Luhmann, Jr., H. K. Park, E. Mazzucato, M. J. van de Pol, I. G. J. Classen, A. J. H. Donné, and R. Jaspers, Rev. Sci. Instrum. **77**, 10E924 (2006).
[3] J. Wang, C. W. Domier, Z. G. Xia, Y. Liang, N. C. Luhmann, Jr., H. Park, T. Munsat, E. Mazzucato, M. J. van de Pol, I. G. J. Classen, and A. J. H. Donné, Rev. Sci. Instrum. **75**, 3875 (2004).
[4] H. Park, E. Mazzucato, T. Munsat, C. W. Domier, M. Johnson, N. C. Luhmann, Jr., J. Wang, I. G. J. Classen, A. J. H. Donné, and M. J. van de Pol, Rev. Sci. Instrum. **75**, 3787 (2004).
[5] B. H. Deng, C. W. Domier, N. C. Luhmann, Jr., D. L. Brower, A. J. H. Donné, T. Ovevaar, and M. J. van de Pol, Phys. Plasmas **8**, 2163 (2001).
[6] R. P. Hsia, W. R. Geck, S. Cheng, W. M. Zhang, C. W. Domier, and N. C. Luhmann, Jr., Rev. Sci. Instrum. **66**, 834 (1995).
[7] H. J. Hartfuss, T. Geist, and M. Hirsch, Plasma Phys. Controlled Fusion **39**, 1693 (1997).
[8] M. A. Van Zeeland, G. J. Kramer, M. E. Austin, R. L. Boivin, W. W. Heidbrink, M. A. Makowski, G. R. McKee, R. Nazikian, W. M. Solomon, and G. Wang, Phys. Rev. Lett. **97**, 135001 (2006).
[9] I. G. J. Classen, J. E. Boom, W. Suttrop, E. Schmid, B. Tobias, C. W. Domier, N. C. Luhmann, Jr., A. J. H. Donné, R. J. E. Jaspers, P. C. de Vries, H. K. Park, T. Munsat, M. Garcia-Munoz, and P. A. Schneider, Rev. Sci. Instrum. **81**, 10D929 (2010).
[10] G. S. Yun, W. Lee, M. J. Choi, J. Kim, H. K. Park, C. W. Domier, B. Tobias, T. Liang, X. Kong, N. C. Luhmann, Jr., and A. J. H. Donné, Rev. Sci. Instrum. **81**, 10D930 (2010).
[11] T. Munsat, C. W. Domier, X. Kong, T. Liang, N. C. Luhmann, Jr., B. Tobias, W. Lee, H. K. Park, G. S. Yun, I. G. J. Classen, and A. J. H. Donné, Appl. Opt. **49**, E20 (2010).
[12] P. Zhang, C. W. Domier, T. Liang, X. Kong, B. Tobias, N. C. Luhmann, Jr., H. Park, I. G. J. Classen, M. J. van de Pol, A. J. H. Donné, and R. Jaspers, Rev. Sci. Instrum. **79**, 10F103 (2008).
[13] G. J. Kramer, C. Z. Cheng, G. Y. Fu, Y. Kusama, R. Nazikian, T. Ozeki, and K. Tobita, Phys. Rev. Lett. **83**, 2961 (1999).